

APPLICATION OF HIGH STABILITY OSCILLATORS TO RADIO SCIENCE EXPERIMENTS USING DEEP SPACE PROBES

E. R. Kursinski
Jet Propulsion Laboratory
California Institute of Technology
Pasadena, California 91109

Abstract

The microwave telecommunication links between the earth and deep space probes have long been used to conduct radio science experiments which take advantage of the phase coherency and stability of these links. These experiments measure changes in the phase delay of the signals to infer electrical, magnetic and gravitational properties of the solar system environment and beyond through which the spacecraft and radio signals pass. The precision oscillators, from which the phase of the microwave signals are derived, play a key role in the stability of these links and therefore the sensitivity of these measurements. These experiments have become a driving force behind recent and future improvements in the Deep Space Network and spacecraft oscillators and frequency and time distribution systems.

Three such experiments which are key to these improvements are briefly discussed here and the relationship between their sensitivity and the signal phase stability is described. The first is the remote sensing of planetary atmospheres by occultation in which the radio signal passes through the atmosphere and is refracted causing the signal pathlength to change from which the pressure and the temperature of the atmosphere can be derived. The second experiment is determination of the opacity of planetary rings by passage of the radio signal through the rings. Because the signal is coherent, the diffraction effects can be removed resulting in resolutions of 10's to 100's of meters in the radial direction depending on a number of factors including the coherence time of the microwave signal. The third experiment is the search for very low frequency gravitational radiation. The fractional frequency variation of the signal is comparable to the spatial strain amplitude the system is capable of detecting. A summary of past results and future possibilities for these experiments are presented.

INTRODUCTION

Microwave telecommunication links between the earth and deep space probes have been used since the beginning of space travel for communication and navigation. The phase stability required for these functions provided the opportunity for radio science experiments measuring changes in the signal phase and group delay to infer electrical, magnetic and gravitational properties of the solar system and beyond. The sensitivity of these measurements is ultimately limited by the precision oscillators from which the phase of the microwave signal is derived. These experiments have become a driving

force behind recent and future improvements in the reference oscillators and frequency distribution systems in NASA's Deep Space Network (DSN) and planetary space probes. The purpose of this paper is provide some insight into the source of these and future requirements.

Three experiments have been chosen for this discussion which collectively push spacecraft and ground oscillator performance. The first is the remote sensing of planetary atmospheres by occultation technique where the radio signal passes through a planet's atmosphere and is refracted causing the optical path length of the signal to change from which the pressure and temperature of the atmosphere can be estimated. The second experiment is the determination of the microwave opacity of planetary rings through the changes in the signal amplitude and phase induced during the signal's passage through the rings. The third experiment is the search for very low frequency gravitational radiation. The fractional frequency variation of the signal is comparable to the spatial strain amplitude of the gravitational waves which the system is capable of detecting.

The instrument consists of the combined radio systems of the spacecraft and ground tracking stations and is operated in one of two configurations. The first is referred to as the "one-way" or noncoherent doppler (or bi-static radar) mode where independent reference oscillators are used at the earth and the spacecraft. In the "two-way" or coherent doppler mode, only an earth-based reference oscillator is used. A coherent signal is transmitted from the earth, received at the spacecraft by a transponder and then retransmitted to the earth. Upon reception at the earth, the signal's frequency is essentially differenced with an estimate of the original transmitted frequency derived from the same reference oscillator. The two-way mode provides the more sensitive measure of signal phase owing to the stability of the hydrogen masers at each DSN tracking complex. However, for the two-way mode to function properly, the transponder must acquire and maintain phase lock on the uplink signal which is difficult when rapid signal dynamics exist making the one-way mode preferable for occultation measurements. This mode places tight requirements on the phase stability of the oscillator on-board the spacecraft.

ATMOSPHERIC OCCULTATIONS

The atmospheric occultation technique was first conceived in the early 1960's and first used to successfully characterize a planetary atmosphere with Mariner IV at Mars [1,2]. It has characterized the pressure and temperature of the atmospheres of all the major bodies in the solar system with the exception of Pluto. This technique is an optics experiment where the atmosphere acts as a lens whose properties are inferred from the perturbations induced in the light passing through it. As viewed from the earth, the spacecraft passes behind the planetary atmosphere and the refraction generated increase in the signal's optical path length is measured *via* the signal phase (see Figures 1 and 2).

Given the atmospherically induced phase shift versus time, as well as an accurate knowledge of the trajectory and gravity field of the planet, the recovery of the atmospheric pressure and temperature proceeds as follows [3]:

1. The asymptotic paths of the signal into and out of the atmosphere are computed based on the bending angle required to generate the measured atmospheric frequency shift.
2. The bending as a function of altitude is transformed into refractivity *vs* altitude via an Abel transform.

3. The number density profile is recovered from the refractivity profile using the fact that the measured refractivity is proportional to the refractivity per molecule times the number of molecules along the signal's path.
4. The pressure is determined by integrating the weight in the column of atmosphere above each altitude and setting the pressure such that it supports this weight (condition for hydrostatic equilibrium).
5. The temperature profile is computed from the equation of state (ideal gas law in the simplest case) using the number density and pressure profiles derived in steps 3 and 4.

Steps 3 and 4 require some knowledge of the average atmospheric constituents which is provided by other instrumentation on the spacecraft and the earth. From these steps it is clear that errors in phase map sequentially into errors in bending angle, refractivity, number density, pressure and temperature. A direct analytical solution of this error propagation does not exist although the author is presently pursuing this task. Simulations have generally been used instead to estimate the effects of the oscillator noise.

The minimum detectable bending angle provides an indication of the sensitivity of the technique. For small bending angles, the doppler shift due to bending is approximately:

$$F_{\text{doppler}} = F_0 \Theta v / c \quad (1)$$

where F_0 is the nominal microwave frequency, Θ is the bending angle in radians, v is the component of the spacecraft velocity in the plane of the sky and c is the velocity of light in a vacuum. The minimum detectable bending angle occurs when this doppler shift exceeds the uncertainty in the signal frequency. Given a 10^{-12} oscillator and a 10 km/sec plane of the sky velocity (typical numbers for Voyager), bending angles as small as 30 microradians can be detected.

In high altitudes, the technique is limited by the presence of sufficient material to cause measurable bending and phase shift. In the Voyager case, a typical upper altitude limit is 0.1 to 1 millibar with temperature uncertainties estimated to be around 10 Kelvin. Figure 3 contains the vertical temperature *vs* pressure profiles for the inbound and outbound occultations of Uranus [4]. One noteworthy exception to this upper limit was the occultation of Triton, the large moon of Neptune, in which the sensitivity was pushed another order of magnitude by least squares fitting the entire measured phase profile to the phase shift due to an isothermal atmosphere. The recovered surface pressure and isothermal temperature of Triton were 16 ± 3 microbars and $48 \text{ Kelvin} \pm 5$ respectively dominated by the uncertainty in the oscillator phase over the ten second occultation [5].

In lower altitudes the trajectory often limits the maximum bending angle where the deepest penetration into the atmosphere occurs. For the Pioneer Venus orbiter, the maximum depth is limited to 40 km above the surface where the bending angle exceeds a critical refraction angle below which the ray does not reemerge from the atmosphere. Absorption by atmospheric constituents such as ammonia can also limit the penetration depth. Maximum pressure levels of a few bars were typically achieved by Voyager.

To first order the pressure and number density (and therefore refractivity) of an atmosphere increase exponentially with decreasing altitude and the dependence is exactly exponential in a region where the temperature is constant (isothermal). This dependence is characterized by a scale height, the change in altitude over which the parameter of interest changes by a factor of e , the base of the natural

logarithm. The sensitivity of the measurements to the oscillator phase uncertainty primarily depends on the refractivity scale height of the atmosphere and the geometry of the occultation. In order to make a useful measurement, the exponential increase in refractivity and therefore signal phase delay as the ray descends through the atmosphere must grow faster than the increase in uncertainty in the estimated oscillator phase. A relevant figure of merit is the stability of the oscillator over the time required for the raypath to descend a scale height in the atmosphere. In the upper atmosphere, this time typically ranges from one to 10 seconds. Deeper in the atmosphere, as the bending increases, the vertical descent of the ray slows significantly. However, the phase delay through this region of the atmosphere is large relative to the oscillator uncertainty and the greatest errors are typically in the upper tenuous regions of the atmosphere as indicated in Figure 3.

Another relevant vertical dimension is the radius of the first Fresnel zone of the occulted ray. This is used as an estimate of the diffraction limited cross section of the geometric ray and sets the vertical resolution of the recovered profiles. In reality, the diffraction can be modeled to some degree and finer vertical structure can be inferred. This sets the maximum signal detection integration time which is typically on the order of 0.1 seconds. Generally both oscillator stability and SNR are limiting factors on this time scale.

The occultation length is also important because it represents the total span over which the signal's phase must be estimated. Shorter, faster occultations are desirable simply because the oscillator phase has less time to wander. Occultation lengths have ranged from 10 seconds for Triton to a few thousand seconds for the large outer planets.

To gain further insight, it is useful to consider the effect of the oscillator phase uncertainty on the altitude at which a certain temperature accuracy can be achieved. The phase uncertainty due to the oscillator must be some small fraction of the phase shift caused by the atmosphere. For each factor of e of improvement in the oscillator's stability, the altitude at which the same phase ratio would be achieved would increase by a scale height. In comparison with the 1×10^{-12} class Voyager oscillator, use of the currently available 1×10^{-13} crystal oscillators [6] would result in an altitude increase of 2.3 ($= \ln(10)$) scale heights assuming a common occultation geometry and spectral shape for the noise. This assumption of similar spectral shape is valid because both oscillator types exhibit flicker frequency noise over the relevant time scales [6]. Given a Voyager-like range of pressure sensitivity from tenths of millbars to a few bars (~ 9 scale heights), this stability would increase the sensitivity to low pressures by an order of magnitude and the total range of altitudes covered by $\sim 25\%$. For a tenuous atmosphere like Mars the increase in altitude range covered would be even more dramatic. Given a 10 km scale height and the expected altitude sensitivity range of 60 km with the 10^{-13} Mars Observer oscillator (Dave Hinson personal communication), a Voyager class oscillator would have reduced this to 37 km indicating the improved performance will result in a 60% increase in the altitudes covered.

Using these same assumptions of common geometry and spectral shape, a similar argument can be made concerning the pressure and temperature uncertainty at any altitude. Assuming that the 5 step process of atmospheric temperature recovery can be represented by an equivalent linear filter, which appears to be the case based on preliminary results by the author, the pressure and temperature uncertainty as a function of altitude will be identical except for the constant scale factor between the noise levels of the two oscillators. Therefore, an improvement of an order of magnitude in the Allan deviation of an oscillator would result in an improvement by this same factor in the accuracy of the recovered pressure and temperature accuracy at all altitudes.

RING OCCULTATIONS

Radio occultations of the ring systems of Jupiter, Saturn, Uranus and Neptune were performed with Voyager of which the Saturnian and Uranian rings provided positive, detailed results. The rings act as huge diffraction gratings whose complex microwave opacities as well as particle densities and size distributions are characterized by the occultation measurements. The opacity measurements are complex in that they provide information on both signal amplitude and phase changes caused by the ring material.

This instrument has a large dynamic range due to the signal to noise ratio (SNR) at the receiver which places limits on sensitivity range and accuracy of the detected opacity profiles [7]. In order to avoid degrading this performance, the signal and receiver local oscillator phase noise spectral densities due to the reference oscillators from which they are generated must be kept below the thermal noise associated with the SNR where possible. The range of Fourier frequencies of interest for Voyager was typically within ± 3 kHz of the carrier frequency covering the angular extent of signal reception by the main lobe of the spacecraft antenna pattern [8].

Concerning diffraction limitations, the uncorrected radial resolution of a radio opacity profile is coarser by factors of hundreds than an optical stellar occultation measurement made with a common viewing geometry due to the relatively long microwave wavelengths. However, the occulted radio signal is coherent allowing the diffraction to be dramatically reduced resulting in resolutions comparable to the optical measurements. Figure 4 shows a near-classic example of a diffraction pattern observed in a ring occultation profile near a sharp edge. Figure 5 provides an excellent example of the effectiveness of the diffraction removal process for Saturn's F-ring. This process has been thoroughly analyzed in [7] and most of what follows is a summary of those results.

This process can be thought of as an inverse transform where the actual opacity of the rings is recovered from the diffraction limited measurements of the opacity. As in the case of a Fourier transform, the finite transform length of the data segment limits the resolution, spatial resolution in this case, of the inversion. A number of factors such as trajectory knowledge and finite antenna pattern footprint on the ring plane can limit the ultimately achievable radial resolution. The achievable resolution is approximately

$$\Delta R_w \cong 2F^2/W \quad (2)$$

where ΔR_w is the radial resolution, F is the Fresnel "scale" and W is the spatial length of the data segment to be inverted. F is radius of the first Fresnel zone in the ring plane divided by square root of 2 and is the characteristic length of a spatial cycle of the diffraction oscillations apparent in the uncorrected occultation results such as those in Figures 4 and 5.

In order for this inversion process to reduce the effects of diffraction, the phase of the unperturbed signal must be known to a fraction of a cycle across the data segment to be inverted. As in the case of an atmospheric occultation, this phase is not precisely known and must be estimated during periods where the direct signal is not visible through the rings. The actual signal phase will gradually wander away from the estimate and at some point the criterion of phase knowledge to a fraction of a cycle can not be maintained. The radial resolution at this point is the resolution ultimately available using this oscillator, essentially by limiting the data segment length in the inversion process.

Having said this, it is important to note that the Saturn and Uranus ring systems are very different

in terms of the radial extent of their individual rings. Saturn has the only ring system in the solar system with microwave opacities over large radial segments such that the direct signal is not be visible for 10's to 100's of seconds during an occultation. In contrast, the Uranian rings are relatively narrow in radial extent separated by large gaps of free space. Typical values range from 2 to 10 km for rings other than the epsilon ring which had a 75 km radial width measured by the egress occultation [9]. These occultations last from a fraction of a second up to a few seconds requiring only that the signal phase be coherent over these relatively short periods.

To provide insight to the relationship between stability and radial resolution, consider the following approximate analysis. An approximate expression relating the coherent integration time, T , and the Allan variance of a reference frequency standard is given by [10]

$$T = 1/[\omega_0 \sigma_y(T)] \quad (3)$$

where $\sigma_y^2(T)$ is the Allan variance and ω_0 is the link frequency in radians per second. The equivalent data segment length corresponds to the radial distance which the raypath moves in the ring plane over this time. Once this width is known, equation 2 can be used to estimate the achievable radial resolution. Figure 6 contains a chart of Allan deviation *vs* integration time, on which four curves are drawn, the Allan deviation performance curves of three oscillators and a line representing phase coherence *vs* integration time for X-band. The radial resolution axis under the integration time axis has been converted from coherence time to effective data segment length and then radial resolution for the Voyager-1 Saturn F-ring occultation geometry. The radial resolution at the intersection of an oscillator performance curve with the coherence curve indicates the oscillator limited resolution providing a simple method for comparing the relative merits of different standards for this application.

A more precise analysis of the effects of oscillator phase noise must consider each noise type (white frequency, flicker frequency etc.) explicitly and must take into account whatever detrending of the phase wander is done in the diffraction removal process. Because it is analytically tractable, the effect of a white frequency noise process on the diffraction removal inversion has been characterized using the phase structure function [7]. The resulting phase limited resolution is:

$$\Delta R_\phi = \Delta R_w \left[\frac{b^2/2}{e^{-b} + b - 1} \right] \quad (4)$$

where $b = \omega_0^2 \sigma_y^2 W / 2\dot{\rho}_0$, $\omega_0 = 2\pi f_0$, $\sigma_y^2(1)$ is the one second Allan variance, W_{eff} is the effective physical width of the data segment to be inverted, and $\dot{\rho}_0$ is the radial velocity in the ring plane. Figure 7 is a plot of equation 4 for different ring occultation geometries at Saturn and Uranus and indicates how the finite oscillator stability degrades the potential radial resolution. The dashed lines in the figure indicate where data processing requirements become prohibitive. The approximate result in Figure 6 provides results within 50% of the white frequency noise estimates in [7].

GRAVITATIONAL WAVE SEARCH

The experiments attempting to detect signatures of very low frequency gravitational radiation in the spacecraft Doppler records place the tightest performance goals on the ground based frequency standards. Theory predicts the presence of distinctive three pulse signatures in the received frequency of

the spacecraft signal produced by the gravitational radiation propagating through the solar system [11]. The instrument is configured in the two-way doppler mode to take advantage of the phase stability of the hydrogen maser frequency standards residing at each DSN tracking complex. It functions essentially as one arm of an interferometer stretched across the solar system. The earth based tracking system at one end is both the transmitting and receiving node of the interferometer and the spacecraft at the other end acts as a reflector. The difference between the frequencies of the transmitted and received signals is generated at the tracking station providing a data set in which to search for 3-pulse signatures.

The instrument's sensitivity is ultimately limited by the stability of the frequency standard over the signal integration time as well as the round trip light time (RTLT) of the signal's passage to and from the spacecraft. The characteristic stability of the hydrogen masers causes the most sensitive region of the instrument to run from approximately 0.0001 to 0.01 Hz where the high frequency limit is set by the thermal noise of the earth-spacecraft microwave link and the lowest detectable frequency by the response function to gravitational radiation (approximately 3/RTLT) [12]. These limits are both tied to the RTLT. A more distant spacecraft such as Pioneer 10 with a 12.25 hour RTLT will have a very low frequency cutoff but also a relatively small high frequency cutoff due to a low SNR.

In terms of detection of gravitational radiation bursts, the Allan deviation of the detrended received signal frequency residuals provides a useful figure of merit indicating the burst strain amplitude sensitivity of the instrument. For sinusoidal sources, the normalized frequency power spectral density provides a relevant figure of merit. A key sensitivity factor is the resolution of the frequency spectrum which can be microhertz or less for data sets acquired continuously over weeks improving the sensitivity to periodic sources over bursts by a factor of 10 or more. The span of continuous data acquisition is typically limited to a few weeks when spacecraft are near solar opposition because the signal phase scintillations due to the interplanetary plasma are minimal [13].

The present system utilizes S-band signals to and from the spacecraft at 2.1 and 2.3 GHz respectively. Measurements made in this configuration in December of 1988 with Pioneer 10 indicate an instrument sensitivity of 2.8×10^{-13} for bursts and a 90% probability of detection for periodic sources of 4×10^{-14} presumably limited by variations in the solar wind [12]. Future measurements will be conducted with higher frequency links to reduce plasma effects. The first measurements will be made using an X-band uplink and downlink (7.1 and 8.4 GHz respectively) system with the Galileo spacecraft in May of 1991. These X-band frequencies should reduce the plasma effects by more than an order of magnitude relative to the S-band system. This first test occurs only 6 months after Galileo's first flyby of the earth. While the relatively short RTLT of this geometry will severely limit the low Fourier frequency sensitivity of the instrument, the SNR will be very high maximizing the high frequency sensitivity. The total contribution of the transmitting and receiving equipment of the DSN in this X-band configuration should be no more than 5×10^{-15} for time scales of 1000 to 3600 seconds with the hydrogen masers contributing no more than 2×10^{-15} [14]. It is also important to realize that stable distribution of the reference frequency over a kilometer or more from a maser to the antenna is not trivial and has led to a research and implementation effort utilizing near-zero temperature coefficient fiber optic cable [15].

A proposal has been written to conduct a Ka-band uplink and downlink experiment (34 and 32 GHz respectively) near the end of the century using the Cassini spacecraft while en route to Saturn. These higher frequencies would reduce the interplanetary plasma instabilities at X-band by another order of magnitude. The potential instrument stability has been estimated as approximately 1×10^{-15} at 1000 seconds [16] with the hydrogen maser performance contribution estimated to be 4×10^{-16} based

on assumed improvements in spin rate selection and magnetic screening as well as phase locking the maser to a trapped ion frequency standard.

OSCILLATOR REQUIREMENTS

These three experiments have been discussed together to provide a sense of the wide range of scales the spacecraft and DSN oscillators must cover. For the two occultation experiments, the spacecraft oscillator must provide stability over time scales covering approximately 7 orders of magnitude from ± 3 kHz on either side of the carrier frequency to durations of more than 1000 seconds. The frequency standards at the DSN tracking complexes must provide stable references over this range as well as still longer spans covering the round trip passage of the signals across the solar system. These time scales are summarized in Figure 8.

FLIGHT OSCILLATORS

The goal for the performance of flight oscillators is really open-ended, the more stable the oscillator, the better the measurements will be. In reality, one must take into account present oscillator technology capabilities in specifying oscillator performance for these experiments. The choice of spacecraft oscillators is very constrained by size, weight, power, reliability and cost considerations which, when combined with the time scales of interest, have thus far made high performance crystal oscillators the references of choice.

In looking to the future, it is interesting to note that with the completion of the Voyager grand tour all planets except Pluto have been visited by spacecraft. Therefore one can expect that most planetary spacecraft will remain at a planet to provide a more in depth characterization of the planet. Orbiting spacecraft must have lower velocities relative to the planets under observation than the Voyagers in order to remain in orbit, implying that future outer planet atmospheric and ring occultations will generally be slower and therefore more sensitive to oscillator phase instability. The Galileo orbiter which will begin orbiting Jupiter in December of 1995 provides an excellent example. The oscillator on board is a spare Voyager oscillator with 10^{-12} performance causing only the first Jovian occultation to rival the Voyager accuracies because the subsequent occultations will be longer and slower.

The Cassini orbiter will characterize the atmospheres of Saturn and Titan and the rings with occultation measurements while in orbit around Saturn. To improve upon the Voyager results, the desire for more accurate atmosphere and ring measurements will of course lead to placing a more stable oscillator on-board. It does appear that this need will be met simply because the Cassini oscillator will presumably have at least the performance of the Mars Observer oscillator. In addition, a stable oscillator will also be placed on the Huygens' probe to provide a stable radio link frequency to measure the velocity of descent of the probe into the Titan atmosphere to characterize winds in the Titan atmosphere.

There are some applications for still longer time scales which haven't been discussed here. Recovery of a planet's gravity field can be accomplished with one-way doppler measurements if the flight oscillator is sufficiently stable. This can be desirable in situations where gravity field and occultation measurements are simultaneous creating a conflict between the desire for the one way versus two way doppler configuration. A related application is the proposed Solar Probe mission which would pass within

a few solar radii of the sun over a 14 hour period making a series of gravity related measurements. The proposed configuration would utilize a flight hydrogen maser to provide the necessary stability. This could also provide an application for a flight trapped ion standard whose performance could conceivably rival that of the maser over this time scale.

GROUND OSCILLATORS

In creating the ground oscillator requirements, it is important to realize that the ground based oscillators can be expected to provide better overall performance than the flight oscillators because they are not limited by the same constraints imposed on the spacecraft equipment. In addition, because of long flight times to the outer planets (such as the seven year trip for Cassini to reach Saturn), ground oscillators can potentially take advantage of more current technology not available when the flight instrumentation was designed and implemented. Therefore the goal of the noise power of ground oscillators in the DSN has been set at 10 dB below that of the downlink signal which is limited by a combination of the flight oscillator, the downlink SNR and any uncalibrated propagation effects. This was achieved for the Voyager Neptune encounter due to the relatively low received signal SNR and the 10^{-12} performance of the 15 year old Voyager oscillator. For Mars Observer (MO), however, the exceptional performance of the flight oscillator will be comparable to that of the hydrogen maser (possibly even exceeding it) for time scales near 1 second making it difficult to achieve this 10 dB goal as indicated in Figures 9 and 10.

TROPOSPHERE

In discussing these requirements it is important to consider other noise sources which can mask the stability of the frequency standards. One particular source worthy of mention here is the phase instability caused by the passage of signals through the earth's troposphere. A simple model of the troposphere indicates a level of instability that, without calibration, will significantly exceed the hydrogen maser stability over time scales less than about a day [17]. A particular case of relevance is the previously mentioned Ka-band gravitational wave search sensitivity estimate which assumes 95% calibration of the troposphere. Present crystal oscillator performance is also becoming comparable to these phase instabilities and will require partial calibration of the earth's troposphere to take full advantage of the oscillator's performance. An interesting application of a very stable flight oscillator has been proposed where the troposphere effects can be removed using simultaneous one and two-way up and downlinks when the flight oscillator stability exceeds the instabilities due to the troposphere [18]. This technique could potentially be applied to all three experiments described here although maintaining the two-way links during the occultations might pose significant technical difficulties. The DSN is presently studying the possibility of deep space tracking stations in orbit around the earth which would potentially eliminate the troposphere from the signal path but would introduce gravity induced orbital perturbations into the signal phase data.

CONCLUSION

In conclusion, I hope that this has provided some insight into these scientific applications and how they utilize phase stability. With the tremendous success of the Voyager radio science experiments which

have proven themselves as powerful tools for characterization of planetary systems and the tantalizing prospect of gravitational radiation detection, these experiments should continue to be a part of future planetary space probes and their symbiotic relationship with the developers of frequency standards should also continue to provide a unique set of applications for future frequency standard research and development.

REFERENCES

- [1] A. Kliore et al., "Occultation Experiment: Results of First Direct Measurement of Mars's Atmosphere and Ionosphere", *Science* 149, 1243–1248, 1965
- [2] G. Fjeldbo and V.R. Eshleman, "The Atmosphere of Mars Analyzed by Integral Inversion of the Mariner IV Occultation Data", *Planet. Space Sci.*, Vol. 16, pp. 1035–1059, 1968
- [3] G. Fjeldbo, A. J. Kliore and V. R. Eshleman, "The Neutral Atmosphere of Venus as Studied with the Mariner V Radio Occultation Experiments", *The Astronomical Journal*, Vol. 76, No.2, pp. 123–140, March 1971
- [4] G. F. Lindal et al., "The Atmosphere of Uranus: Results of Radio Occultation Measurements With Voyager 2", *Journal of Geophysical Research*, Vol. 92, No. A13, pp. 14987–15001, December 30, 1987
- [5] G. L. Tyler et al., "Voyager Radio Science Observations of Neptune and Triton", *Science*, Vol. 246, pp. 1466–1472, 15 December 1989
- [6] J. R. Norton, "Ultrastable Quartz Oscillator for Spacecraft", Proc. of 21st Annual Precise Time and Time Interval Planning Meeting (PTTI), Nov. 28–30, 1989, pp. 509–518
- [7] E. A. Marouf, G. L. Tyler and P. A. Rosen, "Profiling Saturn's Rings by Radio Occultation", *Icarus*, Vol. 68, pp. 120–166, 1986
- [8] E.R. Kursinski and S.W. Asmar, "Radio Science Ground Data System Requirements for the Voyager Neptune Encounter", submitted to The Telecommunications and Data Acquisition Progress Report Dec. NASA JPL Pasadena California
- [9] D. L. Gresh et al., "Voyager Radio Occultation by Uranus' Rings. I: Observational Results", *Icarus*, Vol. 78, pp. 131–168, 1989
- [10] W.K. Klemperer, "Long-baseline radio interferometry with independent frequency standards", Proc. IEEE, vol. 60, pp. 602–609, May 1972
- [11] F.B. Estabrook and H.D. Wahlquist, GRG 6, 439 (1975)
- [12] J. D. Anderson et al., "Application of Hydrogen Maser Technology to the Search for Gravitational Radiation", Proc. of 21st Annual Precise Time and Time Interval Planning Meeting (PTTI), Nov. 28–30, 1989, pp. 259–268
- [13] J. W. Armstrong, R. Woo and F. B. Estabrook, "Interplanetary Phase Scintillation and the Search for Very Low Frequency Gravitational Radiation", *The Astrophysical Journal*, Vol. 230, pp. 570–574, June 1, 1979

- [14] E.R. Kursinski, "High Stability Radio Links", NASA Conference Publication 3046: Relativistic Gravitational Experiments in Space, June 28-30, 1988, pp. 171-178
- [15] P. F. Kuhnle, "NASA/JPL Deep Space Network Frequency and Timing", Proc. of 21st Annual Precise Time and Time Interval Planning Meeting (PTTI), Nov. 28-30, 1989, pp. 479-490
- [16] A.L. Riley et al., "Cassini Ka-band Precision Doppler and Enhanced Telecommunications System Study", Jointly sponsored by NASA/JPL, Pasadena CA, USA and Agenzia Spaziale Italiana, Roma, Italia, Jan. 22, 1990, pp. 13-20
- [17] R. N. Truehaft, "Tropospheric Limitations to the Stability of Radio Metric Delay Measurements", Proc. of 21st Annual Precise Time and Time Interval Planning Meeting (PTTI), Nov. 28-30, 1989, pp. 233-238
- [18] R.F.C. Vessot and M.W. Levine, "A Time Correlated Four-Link Doppler Tracking System", A Close-up of the Sun, ed. M. Neugebauer and R.W.Davies, JPL Publication 78-70, pp. 457-497, Sept. 1978
- [19] E.A. Marouf and G.L. Tyler, "Microwave Edge Diffraction by features in Saturn's Rings: Observations with Voyager 1", Science, Vol. 217, no. 4556, pp. 243-245, July 16, 1982
- [20] G. L. Tyler et al., "The Microwave Opacity of Saturn's Rings at Wavelengths of 3.6 and 13 cm from Voyager 1 Radio Occultation", Icarus, Vol. 54, pp. 160-188, 1983

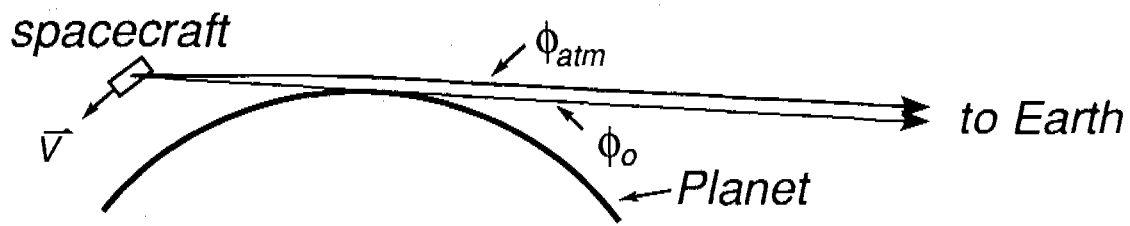


Figure 1: Atmosphere occultation geometry

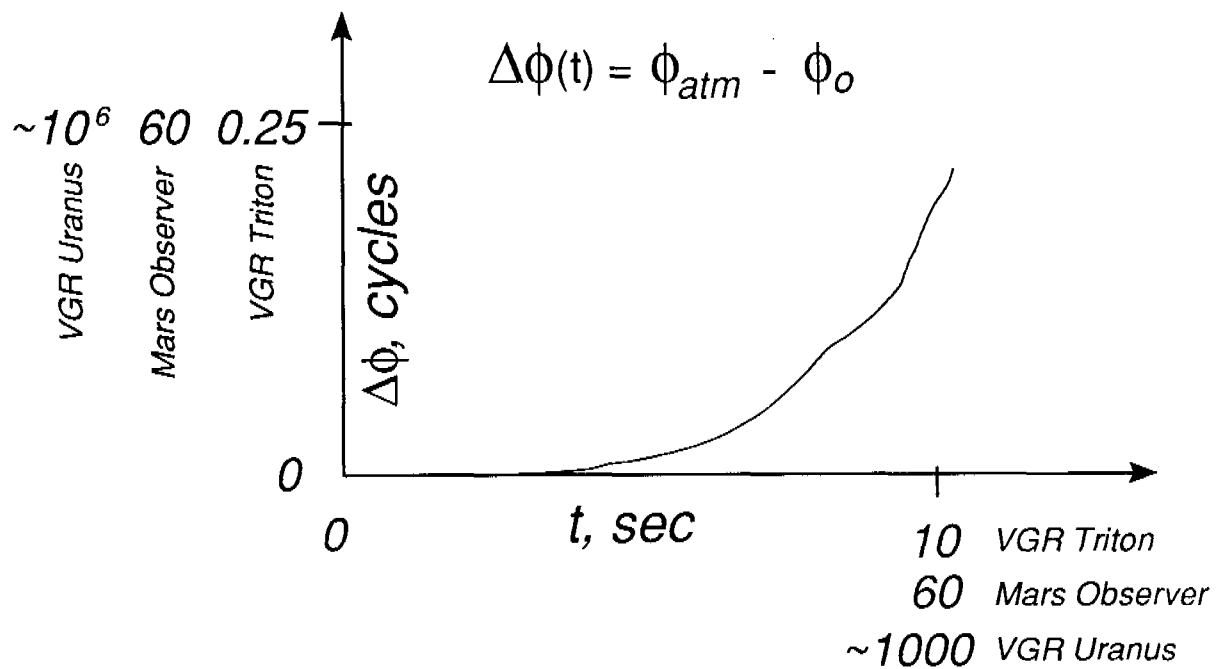


Figure 2: Atmosphere induced phase shift

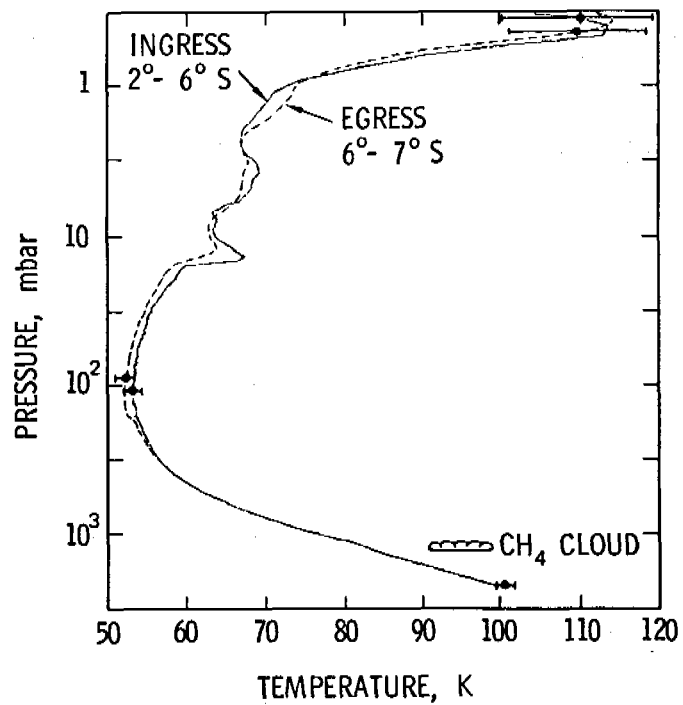


Figure 3: Vertical temperature vs pressure profile for Uranus recovered from radio occultation measurements (Figure from [4])

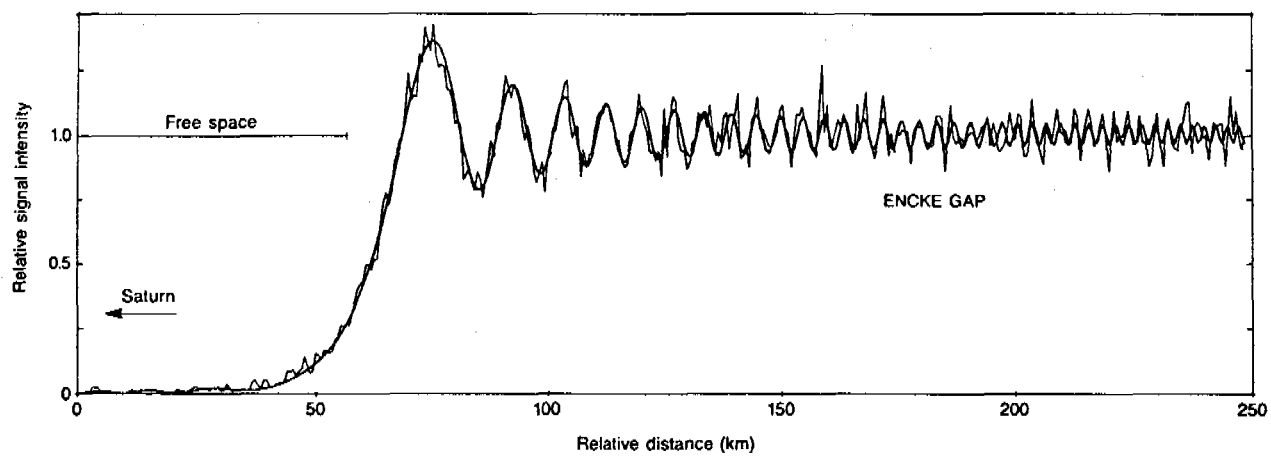


Figure 4: Diffraction effects in radio occultation data caused by the edge of Saturn's Encke gap. Smooth curve shows theoretical diffraction from abrupt edge fitted to irregular curve of measured signal intensity. (Figure from [19])

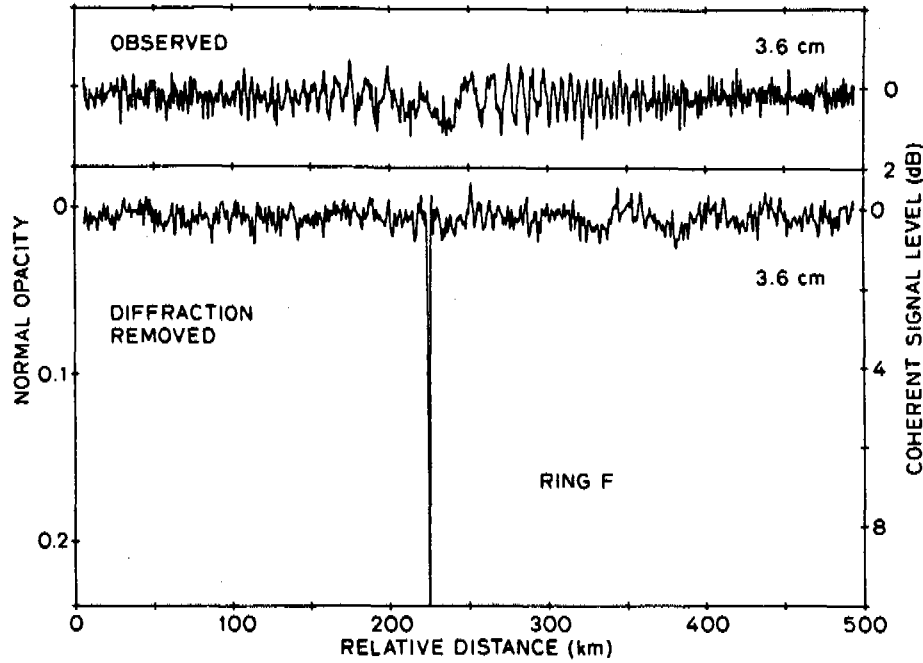


Figure 5: Effect of diffraction removal on observed opacity of Saturn's F-ring (Figure from [20])

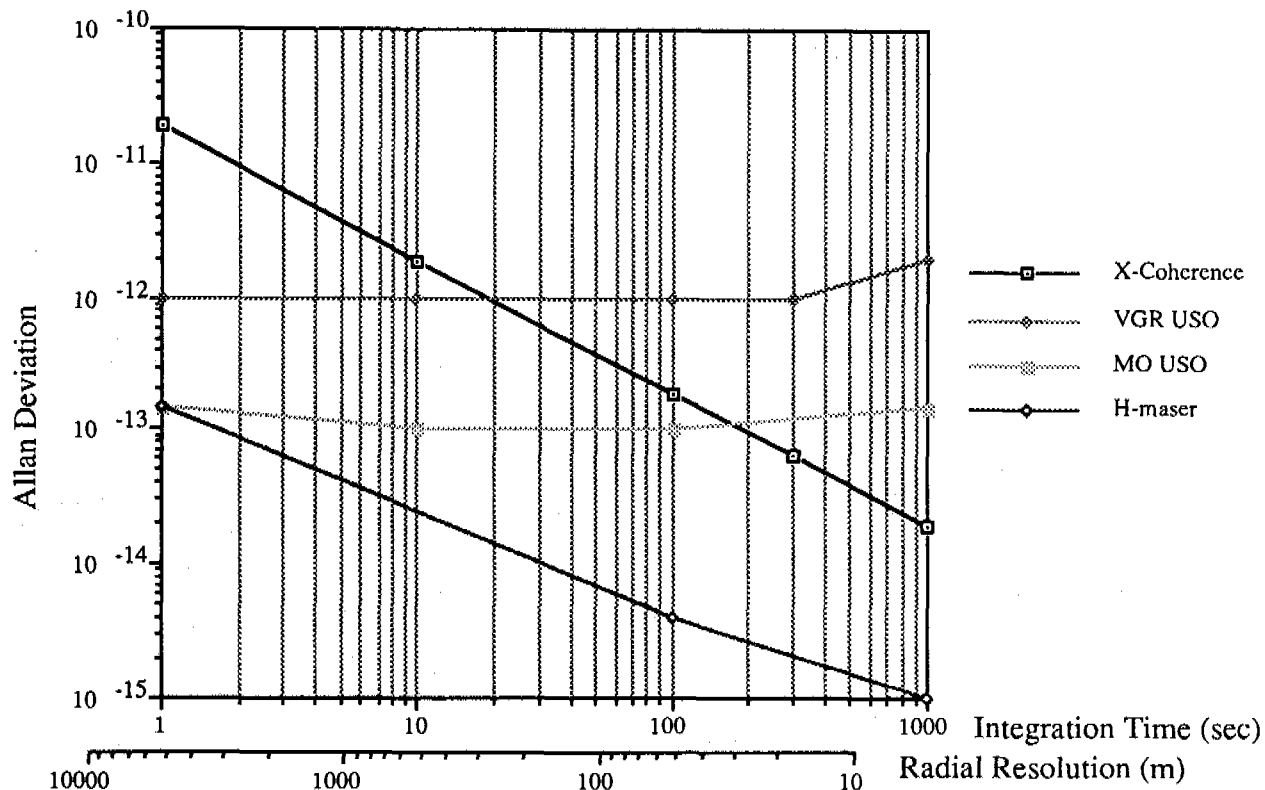


Figure 6: Limitation of Saturn F-Ring radial resolution at X-band due to oscillator stability

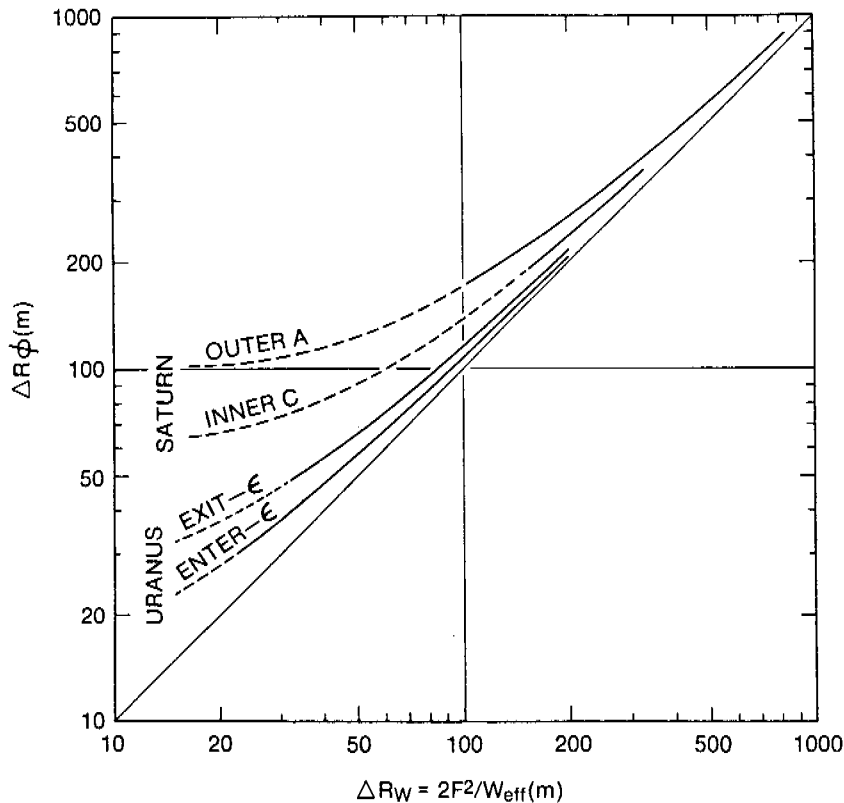


Figure 7: Comparison of the limitation of oscillator phase instability on the radial resolution of recovered ring opacity profiles for the cases of Voyager 1 at Saturn and Voyager 2 at Uranus assuming white frequency noise with $\sigma_y(1)=4 \times 10^{-12}$. At Saturn, the phase instability limiting resolution is about 200 m. At Uranus, this limit is about 30 and 45 m at occultation entry and exit of the epsilon ring. The difference is due to the different occultation geometries for the two planets. (Figure from [7])

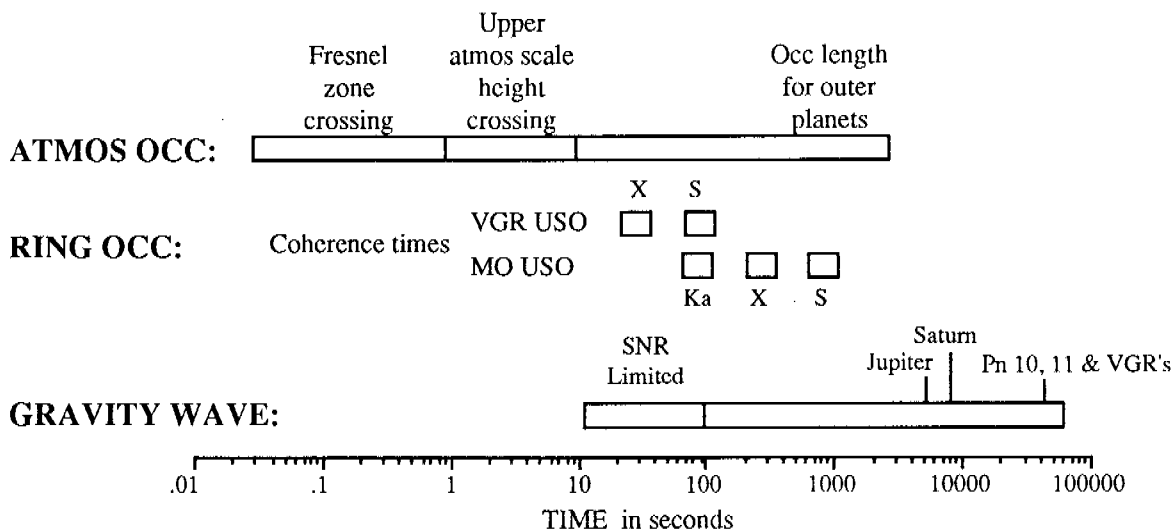


Figure 8: Time Scales of Interest

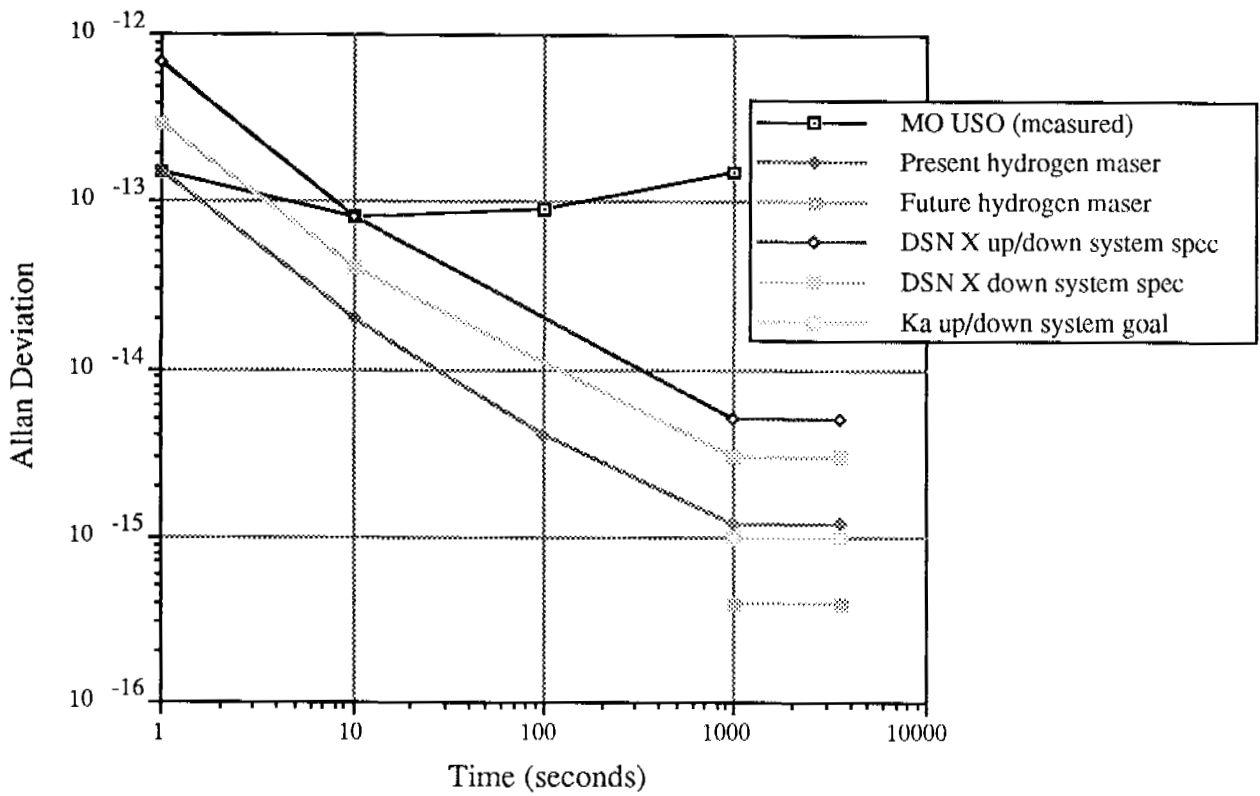


Figure 9: Present and Future Stability Performance

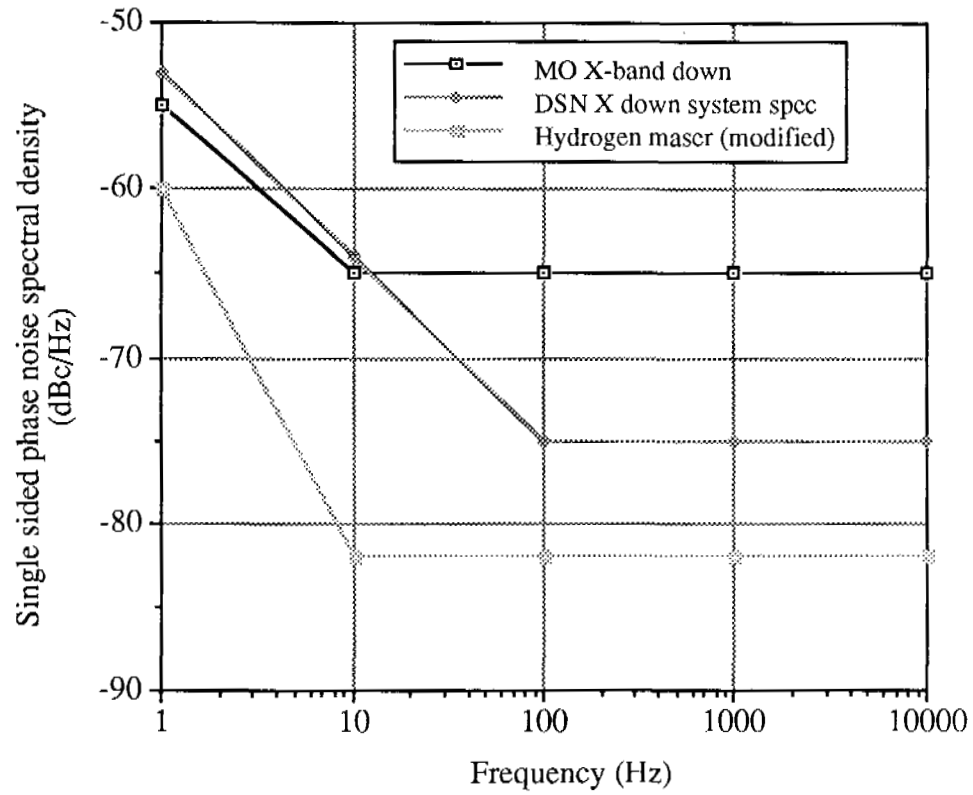


Figure 10: Spectral Purity Performance